HOT STREAK EVOLUTION IN AN AXIAL HP TURBINE STAGE

P. Gaetani - G. Persico
LFM, Energy Dept., Politecnico di Milano, Via Lambruschini, 4, 20158 Milano - Italy
paolo.gaetani@polimi.it
www.lfm.polimi.it

ABSTRACT

The paper presents the results of an experimental study on the evolution of hot streaks generated by gas turbine burners in an un-cooled high-pressure turbine stage. The prescribed hot streaks were streamwise directed and characterized by a 20% over-temperature with respect to the main flow at the stage inlet. The hot streak was injected in four different circumferential positions with respect to the stator blade. Detailed temperature and aerodynamic measurements upstream and downstream of the stage, as well as in-between the blade rows were performed. Measurements showed a severe temperature attenuation of the hot streaks within the stator cascade; some influence on the aerodynamic field was found, especially on the vorticity field, while the temperature pattern resulted severely altered depending on the injection position. Downstream of the rotor, the jet resulted spread over the pitch above midspan and more concentrated at hub. Rotor secondary flows were also enhanced by hot streaks.

KEYWORDS

HOT-STREAKS, AXIAL TURBINE, TURBINE PERFORMANCE, TURBINE-COMBUSTOR COUPLING

NOMENCLATURE

AR = aspect ratio
Cpt_R = relative total pressure coeff.,

$$Cpt_R = \frac{Pt_R - Patm}{Pt_{in} - Patm}$$

$c_{x,V}$ = Vane axial chord
D_M = mean diameter
G = mass flow rate
h = blade height
HSG = Hot Streak Generator
Y = total pressure loss, $Y = \frac{Pt_{in} - Pt_{out}}{Pt_{out} - P}$
n = rotational speed
N_b = blade number
NV (PV) = Negative (Positive) Vorticity Core
r = radius
t_c = trailing edge thickness
TLV = Tip Leakage Vortex
TPV (HPV) = Tip (Hub) Passage Vortex
T_s = static temperature
TSV = Tip Shed Vortex
T_T = total temperature
V = absolute velocity
α = absolute flow angle, from axial
β = total to static expansion ratio
δ = deviation angle
σ = solidity
Δθ = geometrical blade deflection
ρ = density
Ωs = streamwise vorticity

Subscripts
h= hub
ref = reference

INTRODUCTION

The optimization of a gas turbine engine is crucially influenced by the combination between the combustor and the high pressure turbine (HPT). The progressive rise in turbine inlet temperature and

the subsequent lower dilution ratio, the reduction of axial extension of the engine and the increased loading of the turbine blades make critical the combustor-turbine matching, resulting in aero-thermal (Sharma et al., 1992, Burtler et al., 1989, Dorney et al. 2000, An et al. 2009) as well as aero-acoustic (Knobloch et al., 2016) issues. The HPT is characterized by inlet total temperature distortions due to the residual traces of the combustor burners, which are normally called 'hot streaks'. Theoretical analyses (Munk and Prim, 1947, Hawthorne, 1974) suggested that the migration of hot streaks in stationary and rotating blade rows should occur according to different mechanisms. In particular, the hot streaks incoming in the turbine stage should be convected throughout the stator channel to be finally released as high-speed jets, which impinge on the rotor blade pressure side and cause a periodic fluctuation of rotor incidence angle. These features might alter significantly the blade surface temperature, with noteworthy implications on the rotor cooling effectiveness (Butler et al., 1989). Besides detailed investigations on the aerothermal features of the flow released by combustors (Andreini et al., 2016 among others), recent studies have considered more realistic configurations, combining the hot streak with a local streamwise vorticity (Jacobi et al., 2016) and studying the potential for clocking between the burners and the stator blades (Koupper et al., 2016).

The residual hot streak entering the rotor induces even more complex features within the rotor blade row, including the generation of further vorticity cores which are pushed towards the endwalls (Giles and Saxer, 1994), altering the wall temperature in these regions and triggering the development of novel cooling techniques (Ong and Miller, 2012). These studies suggest that the evolution of the hot streaks within the two cascades involves complex phenomena, which have relevant effects also on the aerodynamics of the HPT; they indicate the need of further experimental studies for a proper understanding of the phenomena involved. To this end, an experimental and computational study on hot streak evolution in a HPT has been recently launched at Politecnico di Milano. This paper presents the results of the first experimental campaign on hot streak migration in the stator and in the rotor of a HPT model, for four different clocking positions between the hot streak and the stator blade, thus providing a unique data-set for flow analysis and computational model assessment.

TEST RIG AND INSTRUMENTATION

Test rig

Measurements were performed in the high-speed closed-loop test rig of the Laboratorio di Fluidodinamica delle Macchine (LFM) of the Politecnico di Milano (Italy). The facility is conceived so that a centrifugal compressor and a cooler provide the flow rate and the incoming conditions for the test section, where a single-stage, engine-representative HP turbine is installed. Full details on the facility and the research turbine can be found in Gaetani et al. (2007a); Table 1 provides relevant information on the turbine geometry, as well as the reference operating condition of the present tests. For this first study on hot-streak migration in the turbine, subsonic conditions were considered (even though measurements in transonic conditions have been recently published in Gaetani et al., 2016). The aerodynamics of the turbine operated in subsonic conditions was extensively studied in the last decade and can be found in Persico et al. (2009), Gaetani et al. (2010), Persico et al. (2012). Briefly, under the expansion ratio of 1.4, the flow condition is subsonic for both the stator and the rotor; to set a reference, the stator outlet Mach number at midspan is 0.6 and the Reynolds is $9*10^5$, based on the stator chord. As an average, the rotor outlet relative Mach number is 0.45 with a Reynolds number of $5*10^5$, based on the rotor chord. A meridional cut of the test section is provided in Figure 1, which also shows the turbine inflow system, composed by an inlet centripetal guide vane and a straightener (honeycomb), followed by a 400 mm long annular duct upstream of the turbine. Within this duct, 2 vane axial chords upstream of vane leading edge, an injectors row was installed to simulate the (steady) hot streaks produced by the gas turbine burners; to impose a simple azimuthal periodicity, one injector out of two stator blades was installed (overall 11 injectors).

The present Hot Streak Generator (HSG) was derived from the Entropy Wave Generator (EWG) developed for indirect combustion noise experiments and presented in Gaetani et al. (2015). For the purposes of the present experiment, the hot streak is generated by injecting a steady stream of hot air

in mechanical equilibrium with the surrounding flow. The selection of the feeding pressure to ensure the optimal injection of the hot flow within the main stream was made after a wide preliminary experimental study on the turbine incoming flow, documented in Gaetani et al. (2015) and Bake et al. (2016). The injection temperature was the maximum achievable with the present HSG device; as it will be discussed in detail in the following, the device allowed to reach 390 K in the core of the hot streak, as measured on a traverse placed one vane axial chord upstream of the vane leading edge.

This temperature peak corresponds to an increase of 20% of the main stream temperature, which is a realistic representation of hot-streak-induced temperature perturbation; just to set a general context, Ong at al. (2012) and Jacoby et al. (2016) documented a temperature ratio of ~ 1.09 while Andreini et al (2016) and Koupper et al. (2016) imposed a ratio greater than 1.5.

The hot streaks were injected at 70% span in stream-wise direction, with the aim of minimizing the injector blockage and of limiting the jet interaction with the vane secondary flows.

Table 1. LFM HP turbine stage geometry

Op. cond.	β	n [rpm]	G [kg/s]	$T_{T,IN}$ [K]
	1.4	7000	3.78	323
Geometry	h [mm]	t_c / h	D_M [mm]	gap/$c_{x,v}$
	50	0.02	350	1.00
Blade rows	N_b	σ	AR	Δθ
VANE	22	1.20	0.83	75.2
ROTOR	25	1.25	0.91	115.3

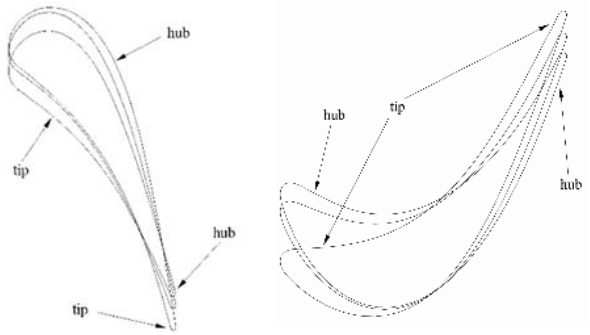

Injectors themselves creates a weak blockage to the turbine mass flow but, thanks to the injected mass flow (that amounts to ~1% of the main stream one), the overall impact of the injection on the mass flow was negligible.

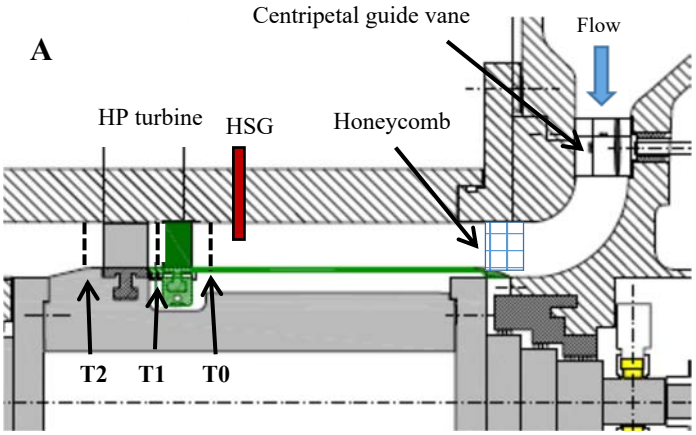

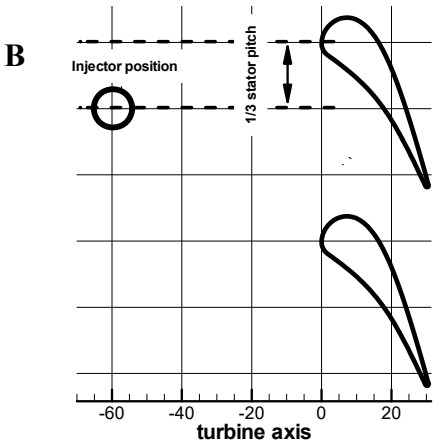

Figure 1A: Meridional cut of the test section; T0 = stator upstream traverse; T1= stator downstream, T2 = rotor downstream

Figure 1B: Injector to stator vane position for PS test point

Instrumentation

The experiments documented in this paper were performed by applying a combination of conventional techniques, namely thermocouple and pneumatic probes, with a Fast-Response Aerodynamic Pressure Probes (FRAPP). The turbine inlet flow was measured with a flattened total pressure probe (probe head dimension 0.5 mm, uncertainty = 60 Pa) and a hot wire probe, both

traversed spanwise one and a half stator axial chord upstream of the stage; in this section a flat profile of uniform total pressure and 2.5% of turbulence intensity were found between 20% and 80%.

Table 2: test matrix

name	Hot streak Azimuthal position
LE	Aligned to the stator leading edge
PS	At 1/3 of the pitch close to the pressure side
MP	At mid pitch
SS	At 1/3 of the pitch close to the suction side

Three-dimensional time-averaged flow measurements downstream of the stator were performed with a 5-hole pneumatic probe (5HP), which features a 1.4 mm head dimension. The probe was placed 32% of the stator axial chord downstream of the stator trailing edge. The 5HP was calibrated in a reference nozzle up to transonic conditions, exhibiting uncertainty of 0.2° in the flow angles and as, maximum, of 0.5% of the local kinetic head for pressures; the uncertainty of the total pressure loss coefficient is 0.2%.

The unsteady flow field downstream of the rotor was measured by a cylindrical single-sensor FRAPP at an axial distance of 32% of the rotor axial chord downstream of the trailing edge. The FRAPP was statically calibrated both in pressure and temperature in order to compensate any thermal drift during the measurement campaign. FRAPP was operated in virtual three-sensor mode and, by applying ensemble averaging in post-processing, the phase-resolved components of flow angle, total pressure and Mach number were measured. The probe was calibrated up to Mach = 0.8 in a reference nozzle resulting in uncertainty of 0.25° on the flow angles and 0.5% of the kinetic head for the pressures. More details on the FRAPP technology can be found in Persico et al., 2005-a. Dedicated dynamic calibration showed a dynamic response of ~80 kHz after digital compensation (Persico et al., 2005-b).

The time-averaged temperature fields were measured by a conventional K thermocouple (joint diameter = 0.25 mm) inserted into a vented probe. The axial positions of the temperature traverse coincide with those pertaining to the 5HP and the FRAPP. The thermocouple was calibrated in a reference oven, resulting in an uncertainty of 0.3 K. Dedicated tests in a calibrated nozzle showed over the Mach number range of interest a substantial invariance of the probe temperature measurement with the flow angle and a recovery factor close to the unity.

Due to mechanical constraints on the turbine casing, probes could be traversed only for one stator pitch in tangential direction. This did not turn out in a penalty for the investigation of the flow upstream and downstream of the stator, because the hot streak evolution remained confined in a single vane passage, as described in the following. On the contrary, it was not possible to investigate the full periodicity over 1/11 of the annular crown downstream of the rotor.

Test matrix

In order to track the hot streak evolution for different azimuthal injection positions, the stator to injector position was varied. Four (4) cases were studied as reported in Table 2.

STATOR INLET CONDITIONS

The stator inlet conditions were measured for all the four injector positions for assessment reasons; however, the large distance between injectors and the vane was sufficient to nullify the impact of the stator on the generation of the hot streaks, which resulted identical for all the cases.

Figure 2 reports the total temperature and total pressure fields upstream of the stator when the hot streak is injected. As the present HSG is based on injection, no hot streak can be generated without a dynamic pressure perturbation. So far, the injector wake and the hot streak produce a non-uniformity in the total pressure distribution (Pmean) which, however, results in a negligible variation of the stage pressure ratio. The temperature ratio between the core of the hot streak and the main stream is 1.2; as well visible in Figure 2 (left frame) the hot streak has an almost circular pattern that smooths down to the main stream temperature.

The Rms of the total pressure (RmsP) evidences the turbulent content of the hot streak, which results from the interaction of the jet with the surrounding flow and from the injector wake itself. The

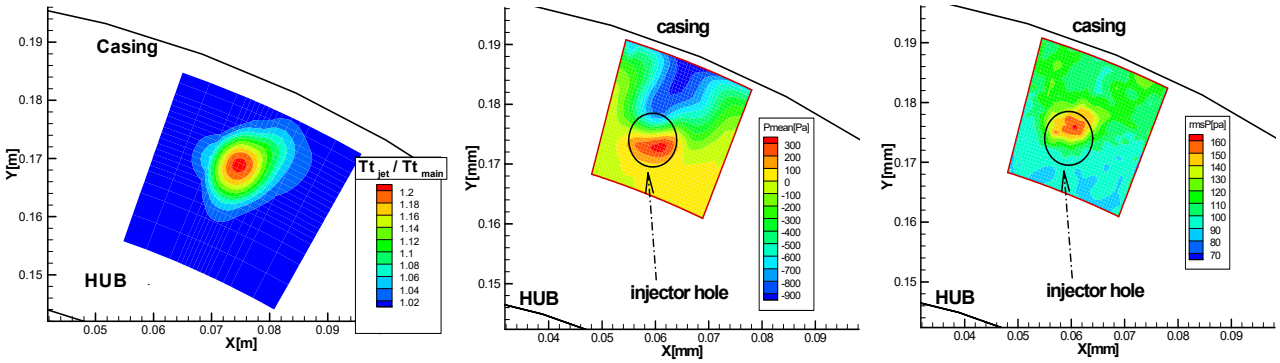

Figure 2: Total temperature and total pressure fields of the hot streak. Pmean is reported as a difference between the local total pressure and the main stream one (kinetic head 1100 Pa)

peak of Rms is located at the upper boundary of the jet where the maximum total pressure gradient is found, namely where the largest shear layer establishes between the injector wake and the hot streak.

STATOR OUTLET FIELD

The stator-exit flow and thermal fields were investigated in dedicated and different tests, after a satisfactory repeatability in the operating condition was assessed. At first, an overview of the thermal field is provided by presenting the results for all the four hot streak positions; then, the flow patterns are discussed in detail and compared in order to show the specific features of each case.

The total temperature field for the different cases is reported in Figure 3; a significant distortion was measured depending on the interaction between the hot streaks and the stator aerodynamics. Moreover, a severe temperature reduction, from 1.2 to 1.05 of the main stream total temperature, is

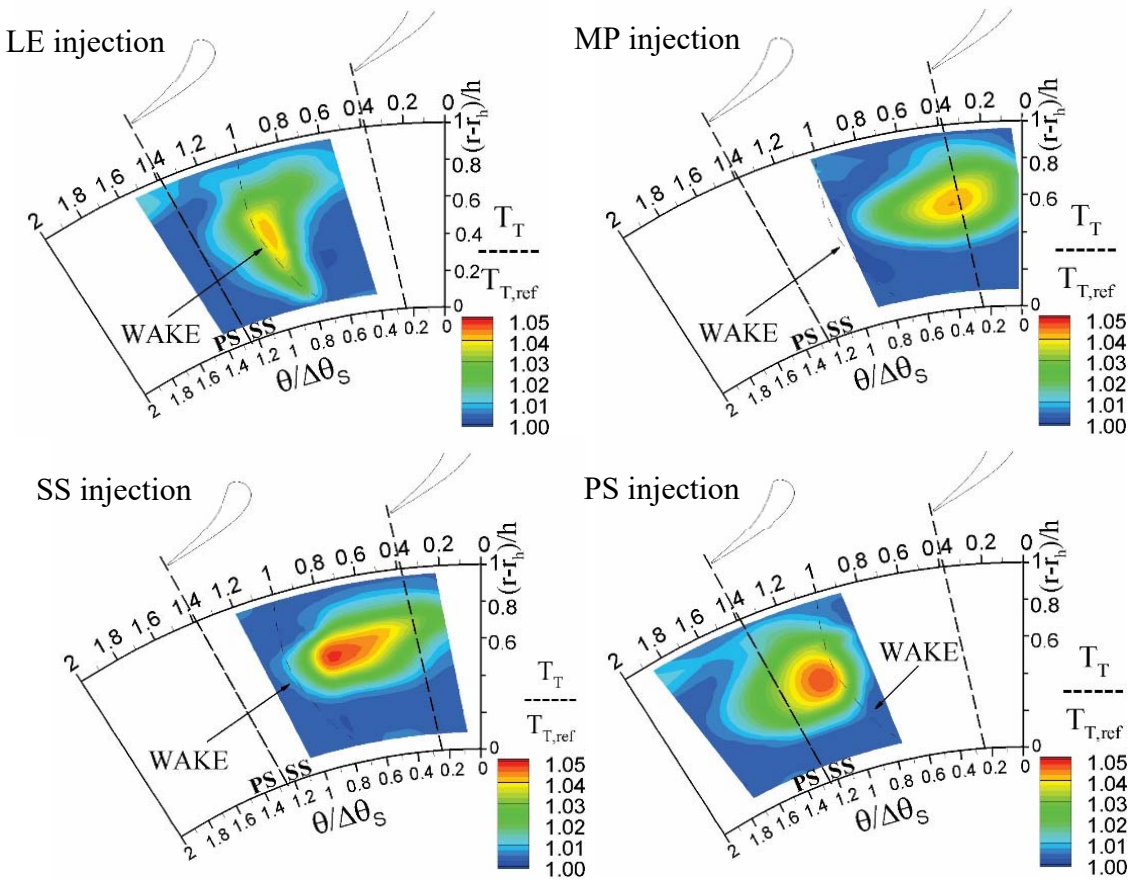

Figure 3: Total temperature fields downstream of the stator for the four hot streak

found as result of the heat exchange with the surrounding flow (and possibly with the blade) and of the diffusion due to turbulence and whirling flows inside the blade channel. For the LE case (top-left frame of Figure 3), the hot streak directly impinges on the stator blade leading edge; the blockage imposed by the blade makes the high temperature zone spread along the blade surface all over the span. In addition, the hot streak undergoes a stretching on the blade suction side (in Figures, it is located on the right hand side of the wake trace) as a consequence of the acceleration and successive deceleration in the blade channel. It is also of interest to note that a temperature increase is found on the tip region towards the suction side of the adjacent blade (top-left corner in each figure); such feature has to be ascribed to the interaction between the hot streak (or, at least, its portion convected on the pressure side surface of the blade) and the cross flow connected to tip passage vortex, that moves part of the hot streak flow along the casing. For the MP case, the hot streak partially interacts with the wake and appears spread over a wide portion of the stator channel. An interaction with the secondary flow is still visible although much weaker than in the LE case.

A slightly higher preservation of the hot streak, resulting in a higher temperature peak, is found when the injection occurs close to the suction and pressure side (SS and PS cases respectively). For the PS case, the entrainment of the hot-streak in the wake and in the cross-flow of the passage vortex is of some importance. Despite the proximity to the wake, it seems that the wake acts as a boundary to the hot streak diffusion. The SS case does not show any peak close to the casing. In fact, the interaction with the passage vortex seems to mainly occur with the under-turning side of the vortex, which is closer to midspan: as a result, the hot area is stretched toward the pressure side of the adjacent blade.

In addition to the tangential displacement, the hot core is also shifted in radial position, as shown in Figure 4, where the upstream profile is also reported. This feature depends on the stator leaning (about 10 degrees towards the pressure side): specifically, in the PS case the hot streak is pushed toward the hub, whereas in the SS case it remains closer to the tip. The MP case is in-between them, while the LE case exhibits a completely different behaviour of the hot streak.

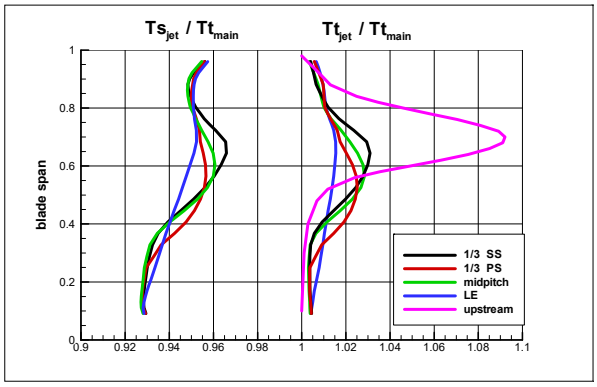

Figure 4: Static and total temperature pitch-wise averaged profile

Beside this description on the hot-steaks intensity and position, a more in-depth discussion and interpretation of the flow features for the different injection positions is reported in the following.

LE Injection Case

For this case, the strongest interaction between jet and blade has been highlighted. The impact of the hot streak on the blade wake can be observed in Figure 5, which reports the total pressure loss coefficients distributions for the reference and the hot streak conditions, as well as their difference.; the wake retains its general width and deficit, even though a small tangential shift is found especially above midspan. The stator-exit vorticity field, not reported for sake of brevity, does not show a specific effect of the hot streak on the stator secondary flow for LE injection (the reader is referred to Gaetani et al., 2016, for a comprehensive discussion of the stator aerodynamics in absence of hot streak injection). Overall, the hot streak injection slightly changes the cascade loss coefficient, especially above midspan (namely, where the jet impinges on the blade), as reported in Figure 6. The tangential shift of the wake is, most probably, connected to the reduction in the mean angle along the blade span (about 1 deg.), also visible in Figure 6, and especially in the radial position corresponding to the core of the hot streak. To assess the flow angle change and the local influence of the hot-streak, the difference in the flow angle between the hot case and the reference one is also reported in Figure

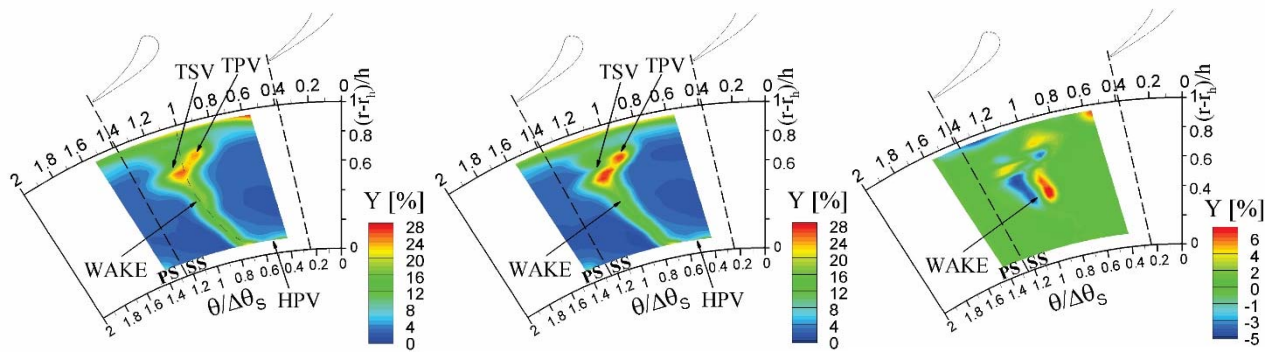

Figure 5: Total pressure loss coefficient at the stator exit for LE hot streak injection. *Left*: no injection; *Center*: with LE injection; *Right*: point to point Y difference (hot streak – ref.)

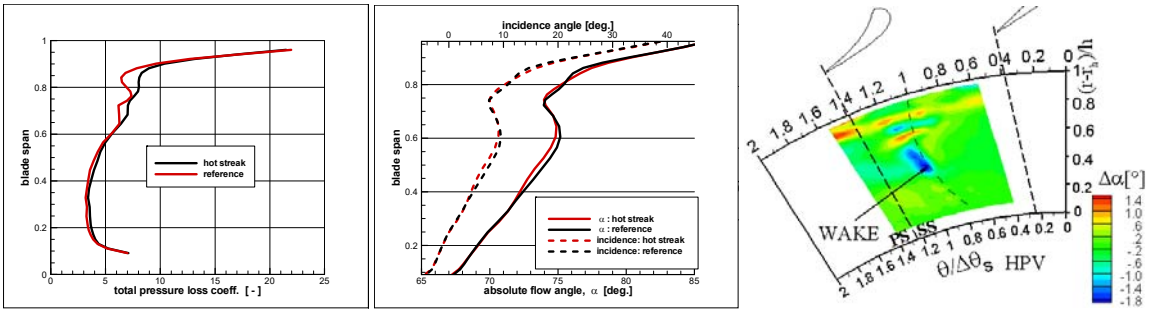

Figure 6: LE injection. *Left*: Y spanwise profile. *Center*: absolute flow angle and rotor incidence spanwise profiles. *Right*: point to point flow angle difference, (hot streak – ref.)

6. Such a change seems to be connected to the increase in the momentum at the stator exit, and also implies a small reduction of rotor incidence angle.

MP Injection Case

A second important case is the mid-pitch injection: this is the case where the minimum interaction between the wake and the hot streak occurs. With reference to the loss coefficient distribution reported in Figure 7, the wake is almost unaffected by the hot streak; very small differences are found only at the boundary of the wake. The pitch-wise averaged profiles, reported in Figure 8, further confirm such conclusion by showing a very small loss increase only concentrated in the tip passage vortex region.

Thanks to the weak interaction with the wake, the hot streak causes some difference in the free-stream area, where a significant change in the flow angle is found between 40% and 70% of the blade span (Fig. 8, centre frame). Such variation is induced by the increase in velocity magnitude which occurs in the hot streak with respect to the reference case, which is also well visible in the right frame of Figure 8 (peak difference of ~10 m/s): as a matter of fact, since the expansion ratio remains constant, any perturbation in the incoming total temperature field induces a velocity change. The change in the flow angle, which becomes more axial, combined with the concurrent increase in the velocity leaves the incidence angle on the rotor almost unchanged.

Induced by the higher velocity of the jet, the streamwise vorticity field - reported in Figure 9 - shows the onset of an additional contribution at the boundary of the hot streak region. As a matter of fact, the higher velocity of the hot streak creates two counter – rotating vorticity just above and below the jet core (being the core centred at 60% of the blade span). The upper one enforces the tip shed vorticity while the lower one stands isolated as a flow structure crossing the whole pitch in tangential direction. The enhancement of the shed vorticity, involves also an increase of the vorticity in the boundary layer, this latter being also related to the injector wake.

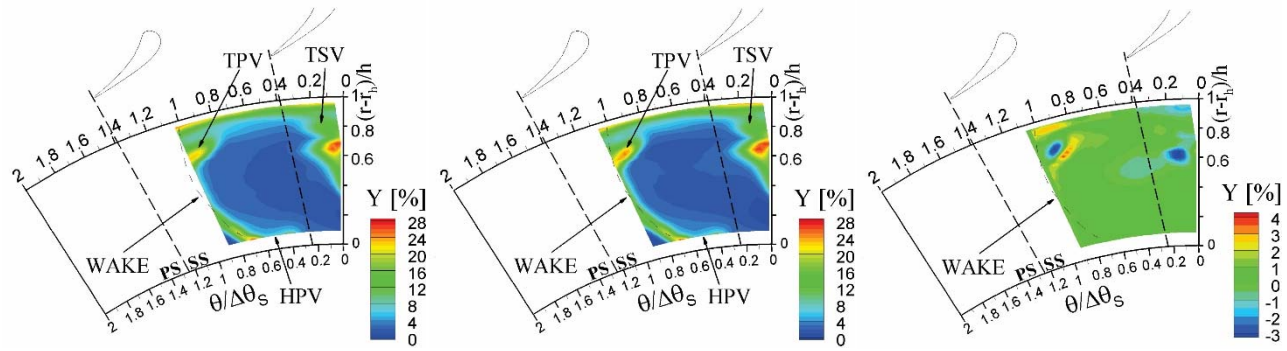

Figure 7: Total pressure loss coefficient at the stator exit for MP hot streak injection. *Left*: no injection; *Center*: with LE injection; *Right*: difference, (hot streak – ref.)

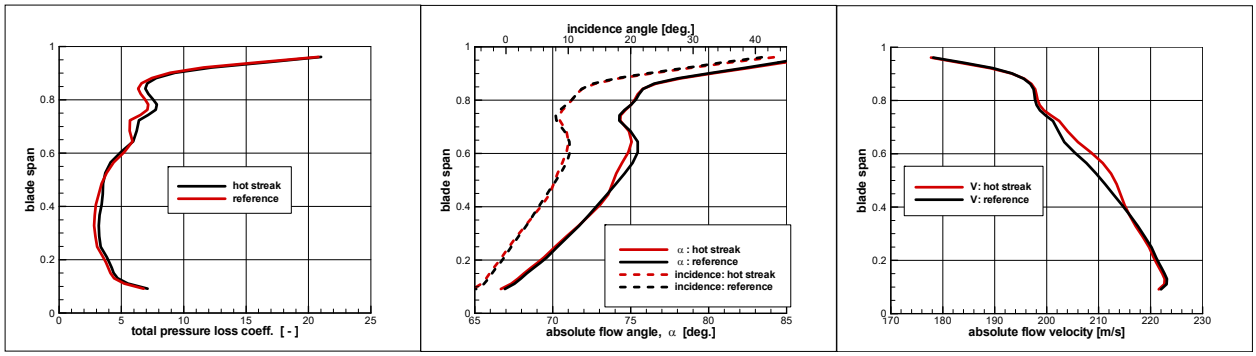

Figure 8: MP injection. *Left*: total pressure loss coefficient spanwise profiles. *Center*: absolute flow angle and rotor incidence spanwise profiles. *Right*: absolute flow velocity spanwise profiles

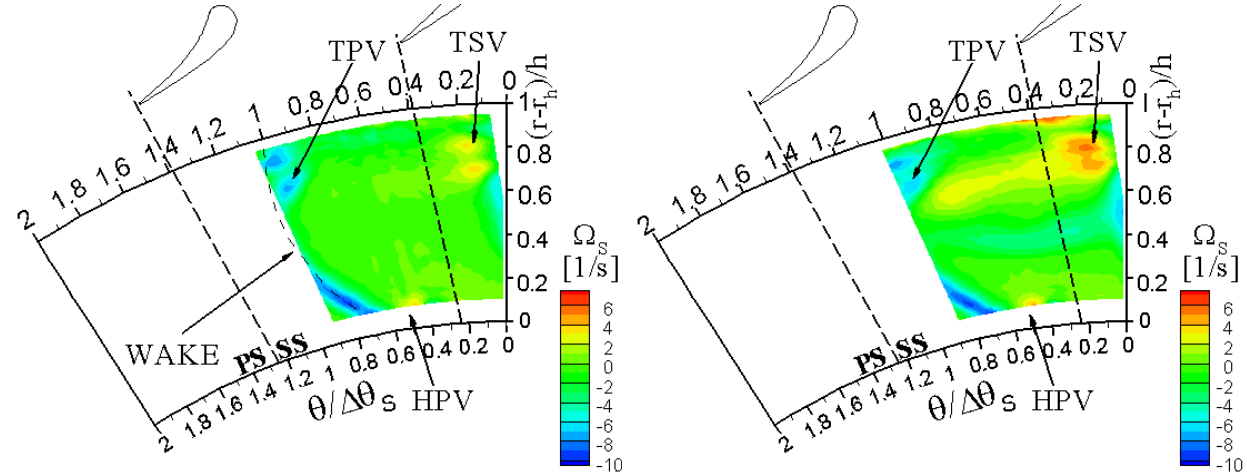

Figure 9: Streamwise vorticity in reference (left) and hot streak (right) cases for MP injection

PS and SS Injection Cases

In case of PS injection, the temperature distribution is similar to the one found for MP injection, although the hot streak is more concentrated and intense, as visible in Figure 3. The impact on the flow angle is also similar to that observed for MP injection, and slightly more intense. A peculiar pattern is found on the vorticity distribution, which is shown in Figure 10 alongside the corresponding reference case. The hot streak seems to induce, also for this case, a significant enhancement of the positive vorticity area (PV) on the pressure side of the wake (where the Tip Shed Vortex (TSV) is

visible also in the reference case). Moreover, as the hot streak is now closer to the wake with respect to MP injection, a more significant interaction with the wake seems to occur in the midspan region, that results in the onset of a local negative vorticity region (NV) at the hot streak bottom margin.

In case of SS injection (Figure 11), the impact of the hot streak on the flow field exhibits the same features observed for the PS case; a similar amplification of vorticity magnitude appears on the other side of the wake, in correspondence of the position of the hot streak. As a result, the vorticity pattern results modified. To conclude, it is interesting to note that, except for the LE injection case, the hot streak induces a systematic effect on the flow field.

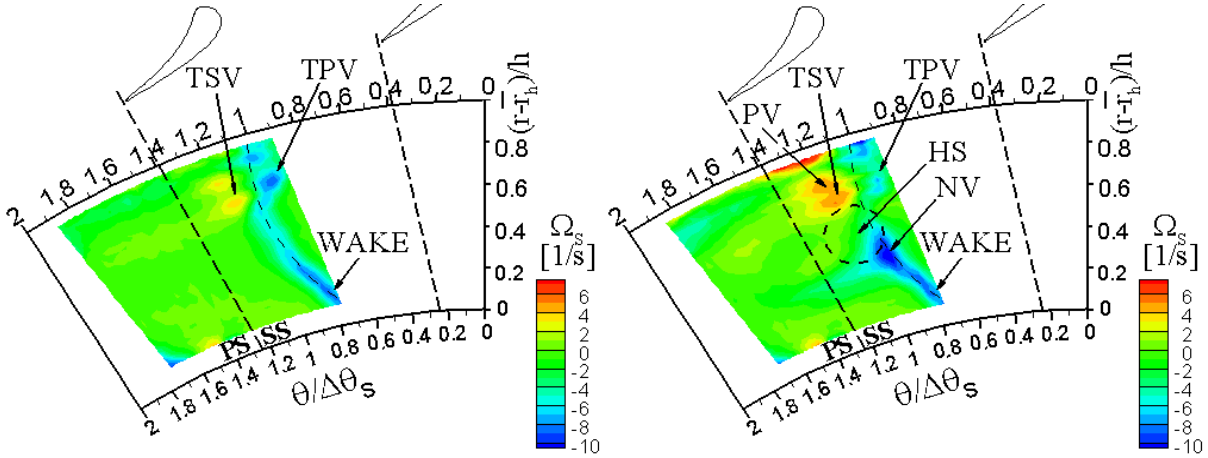

Figure 10: Streamwise vorticity in reference (left) and hot streak (right) cases for PS injection

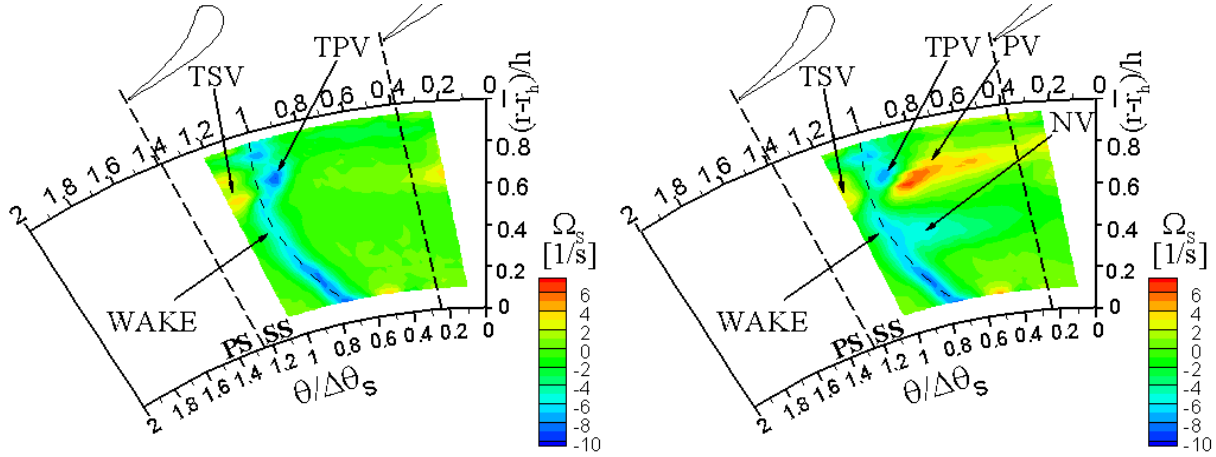

Figure 11: Streamwise vorticity in reference (left) and hot streak (right) cases for SS injection

Stator performance

The overall effect of the hot streak injection on the stator performance is weak for all the 4 cases. In fact, given a total pressure loss coefficient of about 5.9 % for the reference condition (Gaetani et al. 2016), the increase on the single stator channel (ΔY%) due to the hot streak injection is within 0.2% to 0.6%, as reported in table 3, i.e. one order of magnitude lower and, for some cases, within the measurement uncertainty. The total temperature increase (ΔTt) is slightly changing with the minimum for the leading edge case, where the hot streak interacts directly with the blade and for this an effect of the heat exchange with the blade wall is expected, even though very difficult to quantify. The increment reported in Table 3 has to be compared with the mean total temperature increase at the stator inlet on the perturbed channel that is equal to 13.5 K, roughly three times of what found downstream of the stator.

The change in the kinetic energy ($\Delta V^2/2$) and in the momentum ($\Delta \rho V^2/2$) are also reported. The kinetic energy increases because of the higher total enthalpy available in the hot streak, and the highest magnitude is found on the pressure side where the hot streaks undergoes lower mixing in the expansion process; on the contrary, the leading edge injection case exhibits the lowest value, due to the interaction with the blade. The momentum, instead, shows a decreasing trend when the hot streak is injected because of the change in the density related to the higher static temperature. The flow angle, given the high solidity, is in fact negligibly affected by the hot streaks, being its modifications within the 5HP uncertainty.

Table 3: overall parameter downstream of the stator: hot streak - reference

Position	ΔY %	ΔTt (°K)	Δ ($V^2/2$) %	Δ ($\rho V^2/2$) %
LE	0.45	3.9	0.3	- 0.8
PS	0.24	4.9	1.5	- 0.0
MP	0.32	4.5	0.9	- 0.4
SS	0.59	4.7	0.4	- 1.0

ROTOR OUTLET FLOW

In order to investigate the effects of the hot streaks on the whole turbine stage, the temperature field downstream of the rotor is now presented. By virtue of FRAPP measurements, the phase-resolved flow field was also measured and it is discussed in the following.

The reference flow field, which is representative for all the cases, was object of a number of previous publications of the same group (Gaetani et al., 2007b; Persico et al., 2012) and it is briefly recalled here.

Reference time mean flow in the rotating frame

To properly discuss the stage-exit flow and temperature fields in the reference case, the time-averaged flow field in the rotating frame, derived from phase-resolved measurements, is first discussed. Figure 12 reports the relative total pressure coefficient (Cpt_R), rotor deviation angle (δ), and absolute flow angle (α) at the rotor exit. The Cpt_R map shows the rotor wake, identified as the region of low total pressure coefficient, broadened and distorted by the secondary losses; the secondary flows are identified on the basis of the Rankine vortex model applied to the δ distribution. The tip region is dominated by the tip leakage vortex (TLV) and the tip passage vortex (TPV), while the midspan region shows a strong hub passage vortex (HPV) radially shifted by the inherent radial-outward migration of the passage vortices and by the Coriolis effect. The absolute flow angle shows an important flow deflection at the hub, mostly due to the cross-flow activated in the rotor blade row.

The time-averaged total temperature field at the stage exit for reference conditions (namely, without hot streak injection) is reported in the left frame of Figure 13. In absence of upstream total temperature gradients, the distribution is dominated by the spanwise variation of work exchange. The flow experiences a reduction in the total temperature at the hub and close to the tip, in correspondence to the regions of higher work exchange connected to cross-flows and secondary flows. The wake avenue coming from the stator slightly alters the circumferential distribution of the work exchange, thus weakening the spanwise gradients in central region of the pitch.

Temperature field

When the hot streak is injected on the stator leading edge (Figure 13, centre), the hot fluid is entrained within the stator wake and, hence, high total temperature regions can be used as markers of the stator wake avenue at the rotor exit. To better highlight the traces of the hot streak, the difference between the two cases is considered and shown in the right frame of Figure 13. The hot streak appears to be spread all over the passage above midspan. At the hub, instead, it creates a hot spot whose extension is the half of the passage while the other portion experiences a weak decrease in the total temperature, suggesting an alteration in the work extraction process. The migration of the hot streak fluid towards the hub is probably promoted by the combined action of the radial equilibrium in the

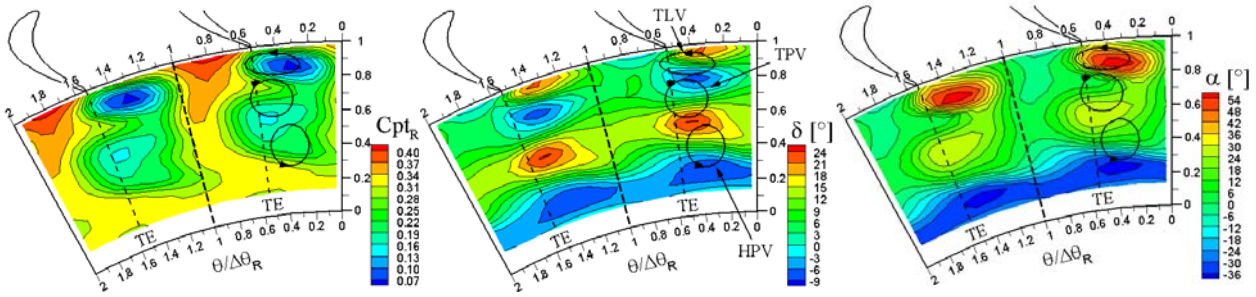

Figure 12: Time-mean flow in the rotating frame for the reference case

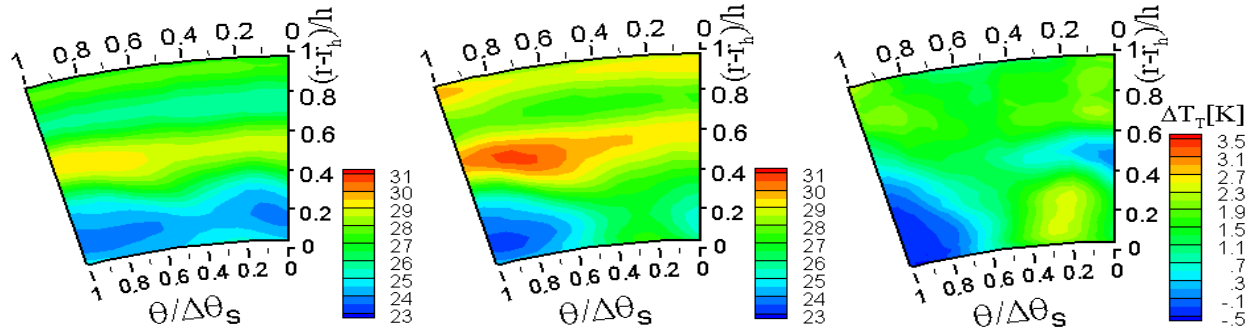

Figure 13: LE injection temperature field. *Left*: total temperature field in reference condition. *Center*: total temperature field in the LE perturbed condition. *Right*: point-to-point difference, (hot streak – ref.)

stator-rotor axial gap and of the rotor secondary flows on the stator wake. Figure 14, reports the results for the MP, SS and PS cases. It is interesting to note that for all these cases, and differently from what observed in Fig. 13, the hot streak appears somehow delimited to the upper part of the channel (namely, where the hot fluid is injected). It should be noted that the periodicity on one stator pitch is not anymore valid, as one injector out of two stator vanes was installed.

As previously described for the MP case, the hot streak location downstream of the stator was in the midspan-tip region and the additional induced vorticity combines with the rotor tip passage vortex one. These features lead to a hot streak spreading in the upper part of the channel with a weak influence on the hub region.

In the PS case, for that the core of the hot streak moved at midspan at the rotor inlet (see Figure 4), the hot fluid interacts also with the rotor hub passage vortex, leading to a stronger effect at the rotor hub. A contribution to the hot streak shift towards to hub may come also from its partial entrainment in the stator wake.

When the hot streak is injected close to the SS, it appears split into two cores at the rotor-exit, one close to the hub and the second one in the tip region. Such unexpected result depends on its position at the rotor entrance: likely, the hot streak portion located in the tip – freestream region is spread by the rotor secondary structures all over the rotor pitch, while the portion that was partially entrained by the wake it is now pushed - inside the rotor - by the centripetal pressure gradient towards the hub.

Time-mean flow field in the rotating frame with hot streaks

Even though the impact of the hot streaks is mainly on the temperature field, some effects of small magnitude are visible also in the rotor aerodynamics, highlighted by FRAPP measurements.

In presence of incoming hot streaks, the flow morphology is modulated depending on the injection position. As a general consideration, the hot streak strengthens and slightly shifts the rotor secondary flows, leading to changes in the flow angle distribution; conversely, negligible effects are detected on the pressure field and the Mach number distribution. Furthermore, as theoretically pointed out by Hawthorne (1974) and computationally predicted by Giles and Saxer (1994) and Ong and Miller

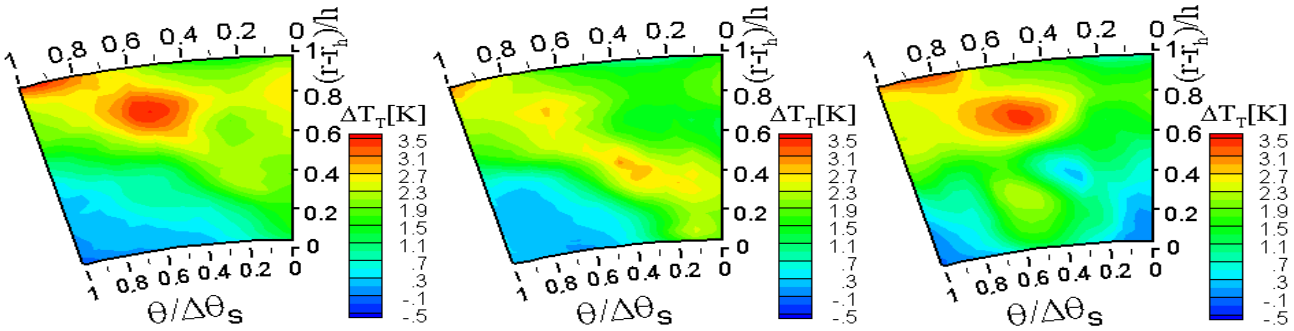

Figure 14: Point-to-point difference with respect to the reference case for: *Left*: MP injection; *Center*: PS injection; *Right:* SS injection.

(2012), the hot streak can alter the generation of secondary vorticity in the rotor. For these reasons, the following analysis focuses on the experimental analysis of the rotor secondary flows and, hence, on the distribution of angles only.

As visible in Figure 15, which reports the point-by-point change between the reference case and those with the hot streak, the largest impact of the hot streak is measured for LE injection. Specifically, the effects of the LE injection consist in the strengthening of the tip leakage vortex and in a general reduction of deviation angle in the midspan region, where the rotor hub passage vortex is found. This has a relevant impact on the absolute flow angle, which globally increases above 60% span and reduces below midspan. These features are probably correlated to the diffused and elongated shape of the hot streak entering the rotor, which result from the noteworthy interaction that establishes between the hot streak and the stator viscous structures in case of LE injection.

The injection at MP, also reported in Figure 15, is characterized by the additional vorticity leaving the stator (enhanced TPV in Figure 9), which is co-rotating to the rotor TPV: as a result, a slight increase of rotor TPV is detected, marked by the increase in spanwise gradient of δ corresponding to the TPV core. No significant change is found in the rotor HPV, which is consistent with the minor traces of the hot streak below midspan at the rotor inlet. However, the MP injection seems to reduce the cross-flow in the region close to the hub, reducing in magnitude both the absolute and relative flow angles. This latter feature is consistent with the temperature field reported in figure 14.

The analysis of the other two cases, reported in the two right frames of Figure 15, confirms the impact of the hot streak position on the rotor secondary flows. In the PS injection case, the effect is more intense also downstream: the secondary flow pattern is slightly shifted below midspan where a clear increase in the deviation angle is found. It is interesting to note that, in the passage vortex

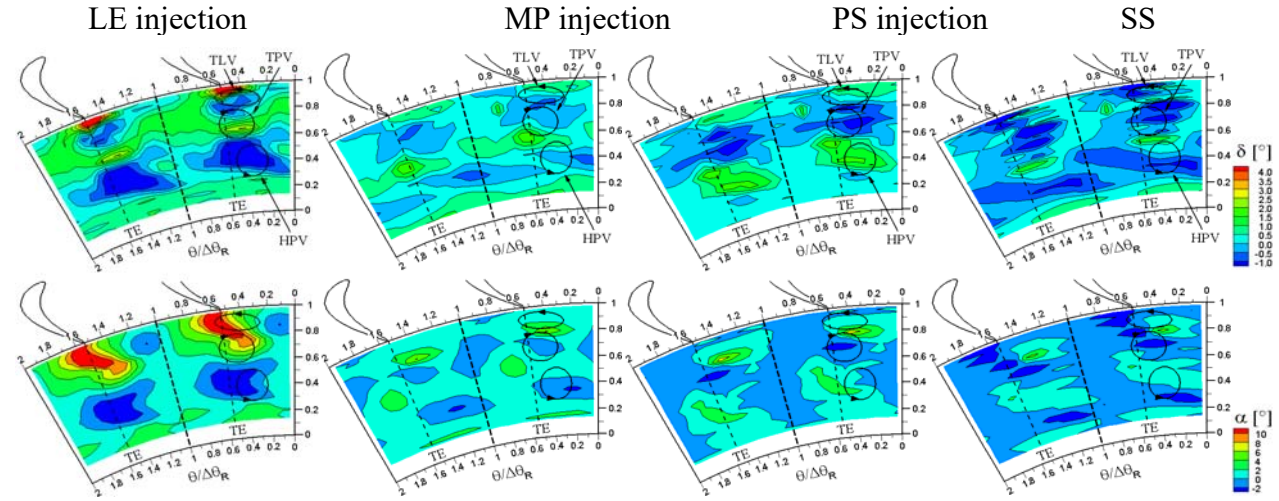

Figure 15: Point-to-point difference of mean flow angles with respect to the reference

regions, the difference in δ measured for PS injection are similar to that observed for LE injection, even though opposite in sign. This is of some significance, considering that the LE injection has a negligible effect on the stator secondary flows, while the PS injection induces a relevant change in the stator-exit vorticity. In case of SS injection, the minimum variation in flow angle is found; this is consistent with the spreading of the hot streak over the entire passage observed on the basis of the temperature field (Figure 14 - right). Moreover, in this case, the stator outlet tip region was not affected, and for this not energized by the hot streak, leading to a lower effect also on the tip leakage vortex

CONCLUSIONS

The paper has presented a comprehensive analysis on the effect of hot streaks migration within a high pressure turbine. Hot streaks were injected in different clocking positions with respect to the stator blade, and provide a total temperature perturbation representative of engine conditions. Several measurements techniques were applied to investigate the hot streak impact on the thermal and aerodynamic behaviour of the stage.

It has been shown that, throughout the convection within the stator channel, the hot streak undergoes different migration and attenuation depending on the injection position. In particular, the clocking of the hot streak with the stator blade leading edge induces a dramatic deformation of the hot streak, which takes the shape of the blade wake. The temperature attenuation across the stator is severe for all the cases, and the maximum temperature ratio drops down from 1.2 to 1.05. With the exception of the injection on the suction side, a portion of the hot streak is entrained in the cross-flow induced by the stator pressure field on the shroud. A negligible increase in the stator total pressure loss is found due to the hot streak transport and evolution.

When the stator blade thermal stress is of concern, the hot streak injection on the leading edge is the worst possible operating conditions, as can be argued by the temperature field downstream of the stator and as already pointed out by other authors (e.g. An Bai-Tao 2009). The MP case seems to guarantee the lowest interaction with the blade and the highest temperature diffusion all over the channel. On the contrary, downstream of the rotor the highest diffusion is found for the PS injection, with potentially positive implications on the following stage.

The expected over-speed induced by the hot streak due to its higher enthalpy content at the stator exit is very limited, although expected also by theoretical analysis as reported in Sharma et al. 1992, and has a minor impact on the rotor incidence angle. Conversely, an interesting effect is found on the vorticity field, which shows additional contributions at the top and bottom of the hot streak (except in the case of leading edge injection). Such additional vorticity cores alter the rotor secondary flows as found at the rotor outlet. The temperature disturbance at the rotor outlet is further attenuated, consistently with a significant spreading of the rotor incoming disturbances. These results are in line with the enhanced migration that the hot streak does experience in the rotating channel, and trigger the interest for further experimental and computational studies specifically oriented to the unsteady hot streak migration in the rotor. Due to the hardware limitations, hampering the flow field analysis over a 1/11 periodicity, no info can be drawn on the stage performance; such limit can be overcome by applying a CFD model, whose thorough validation is presently ongoing thanks to the wide set of data presented and discussed in this paper.

ACKNOWLEDGEMENTS

The present research is a follow up of the RECORD project, grant agreement no. 312444 and funded by the European Union Seventh Framework Program (FP7/2007- 2013).

REFERENCES

Andreini A., Bacci T., Insinna M., Mazzei L., Salvadori S., (2016), *Hybrid Rans-les modelling of the aero-thermal field in an annular hot streak generator for the study of combustor -turbine interaction*, Proceedings of ASME Turbo Expo 2016, GT2016-56583, Seoul, South Korea.

An Bai-Tao, Liu Jian-Jun, Jiang Hong-De, (2009) *Numerical Investigation on Unsteady Effects of Hot Streak on Flow and Heat Transfer in Turbine Stage*, J. Turbomachiney, Vol. 131 pp. 031015-1 - 031015-15.

Bake F., Gaetani P., Persico G., Neuhaus L., Knobloch K., 2016, *Indirect Noise Generation in a High Pressure Turbine Stage*, 22nd AIAA CEAS Aeroacoustics conference, 2016.

Butler, T. L., Sharma, O. P., Joslyn, H. D., and Dring, R. P., (1989), *Redistribution of an Inlet Temperature Distortion in an Axial Flow Turbine Stage*, J. Propul. Power, 5, pp. 64–71.

Dorney D. J., Sondak D.L., (2000), *Effects of Tip Clearance on Hot Streak Migration in a High Subsonic Single Stage Turbine*, J. Turbomachinery, Vol. 122 pp. 613-620.

Gaetani P., Persico G., Dossena V., Osnaghi C., (2007 - a), *Investigation of the Flow Field in a HP Turbine Stage for Two Stator-Rotor Axial Gaps: Part I – 3D time average flow field*, ASME J. of Turbomachinery, Vol. 129, pp. 572-579.

Gaetani P., Persico G., Dossena V., Osnaghi C., (2007 - b), *Investigation of the Flow Field in a HP Turbine Stage for Two Stator-Rotor Axial Gaps: Part II –Unsteady Flow Field*. ASME J. of Turbomachinery, Vol. 129, pp. 580-590.

Gaetani P., Persico G., Osnaghi C. (2010) *Effects of Axial Gap on the Vane-Rotor Interaction in a Low Aspect Ratio Turbine Stage*, pp 325-334, AIAA J. of Propulsion and Power, ISSN 0748-4658, Vol. 26, n° 2, March-April 2010.

Gaetani P., Persico G., Spinelli A., Sandu C., Niculescu F., (2015), *Entropy wave generator for indirect combustion noise experiments in a high-pressure turbine*, 11th European Turbomachinery Conf., Madrid, Spain.

Gaetani P., Persico G., Spinelli A., Mora A., (2016), *Impact of the Expansion Ratio on the Unsteady Aerodynamics and Performance of a HP Axial Turbine*, Proceedings of ASME Turbo Expo 2016, GT2016-56650, Seoul, South Korea.

Giles M. B., Saxer A. P., (1994), *Predictions of Three-Dimensional Steady and Unsteady Inviscid Transonic Stator/Rotor Interaction With Inlet Radial Temperature Nonuniformity*, J. of Turbomachinery, Vol. 116, pp. 347-357.

Hawthorne, W. R., (1974), *Secondary Vorticity in Stratified Compressible Fluids in Rotating Systems*, University of Cambridge, Department of Engineering, Report No. CUEDA-Turbo TR63.

Jacobi S., Mazzoni C., Chana K., Rosic B., (2016), *Investigation of unsteady flow phenomena in the first vane caused by the combustor flow with swirl,* Proceedings of ASME Turbo Expo 2016, GT2016-57358, Seoul, South Korea.

Knobloch K., Neuhaus L., Bake F., Gaetani P., G. Persico G., (2016), *Experimental assessment of the noise generation and transmission in a high – pressure transonic stage* Proceedings of ASME Turbo Expo 2016, GT2016-57209, Seoul, South Korea.

Koupper C., Bonneau G., Gicquel L., (2016), *Large eddy simulation of the combustor turbine interface: study of the potential and clocking effects*, Proceedings of ASME Turbo Expo 2016, GT2016-56443, Seoul, South Korea.

Munk, M., and Prim, R. C., (1947), *On the Multiplicity of Steady Gas Flows having the Same Streamline Pattern*, Proc. Natl. Acad. Sci. U.S.A., 33(5), pp. 137–141.

Ong J., Miller R.J., (2012), *Hot Streak and Vane Coolant Migration in a Downstream Rotor*, J. of Turbomachinery, Vol. 134, pp. 051002-1—051002-10

Persico G., Gaetani P. Guardone A., (2005-a) "*Design and analysis of a new concept fast-response pressure probes*" Meas. Sci. Technol. Vol. 16, pp 1741-1750.

Persico G., Gaetani P. Guardone A., (2005-b) *Dynamic calibration of fast-response probes in a low pressure shock tube*, Meas. Sci. Technol. Vol. 16, pp 1751-1759

Persico G., Gaetani P., Osnaghi C. (2009), *A parametric study of the blade row interaction in a high pressure turbine stage*, ASME J. of Turbomachinery, Vol. 131, pp. 031006-1, 031006-13

Persico G., Mora A., Gaetani P., Savini M., (2012) *Unsteady Aerodynamics of a Low Aspect Ratio Turbine Stage: Modeling Issues and Flow Physics*, ASME J. of Turbomachinery, Vol. 134, 061030

Sharma O.P., Pickett G.F., and Ni R.H., (1992), *Assessment of Unsteady Flow In Turbines*, J. Turbomach., Vol. 114, pp. 79-90.